

Massive MIMO and NOMA Bits-per-Antenna Efficiency under Power Allocation Policies

Thiago A. Bruza Alves, Taufik Abrão

State University of Londrina (UEL), Department of Electrical Engineering, Londrina-PR, Brazil.

Abstract—A comparative resource allocation analysis in terms of received bits-per-antenna spectral efficiency (SE) and energy efficiency (EE) in downlink (DL) single-cell massive multiple-input multiple-output (mMIMO) and non-orthogonal multiple access (NOMA) systems considering a BS equipped with many (M) antennas, while K devices operate with a single-antenna, and the loading of devices $\rho = \frac{K}{M}$ ranging in $0 < \rho \leq 2$ is carried out under three different Power Allocations (PA) strategies: the inverse of the channel power allocation (PICPA), a modified water-filling (Δ -WF) allocation method, and the equal power allocation (EPA) reference method. Since the two devices per cluster are overlapped in the power domain in the NOMA system, the channel matrix requires transformation to perform the zero-forcing (ZF) precoding adopted in mMIMO. Hence, NOMA operating under many antennas can favor a group of devices with higher array gain, overcoming the mMIMO and operating conveniently in the higher loading range $0.6 < \rho < 2.0$. In such a scenario, a more realistic and helpful metric consists in evaluating the area under SE and EE curves, by measuring the bit-per-antenna and bit-per-antenna-per-watt efficiency, respectively. Our numerical results confirm a superiority of NOMA w.r.t. mMIMO of an order of 3x for the SE-area and 2x for the EE-area metric.

Index Terms—Non-Orthogonal Multiple Access (NOMA); massive Multiple-Input Multiple-Output (mMIMO); Energy Efficiency (EE); Spectral Efficiency (SE).

I. INTRODUCTION

The beyond Fifth Generation (5G) of wireless communication systems must allow ultra-dense connections with vastly heterogeneous requirements. The challenges in networks persist, including the Spectral Efficiency (SE) and the Energy Efficiency (EE) joint improvement, the increase in the SE-EE trade-off, and Quality of Service (QoS), always aiming to meet the growing number of devices connected to the network. Among the proposals to solve these challenges, the massive Multiple-Input Multiple-Output (mMIMO) system is the primary proposed system that allows the increase of the link capacity, exploring the propagation of multiple paths with the use of a large number of antennas at the Base Station (BS) [1], [2]. Another relevant enabling technology is the Non-Orthogonal Multiple Access (NOMA), which explores the power domain as an alternative way in terms of multiple access technology, helping to mitigate the spectrum exhaustion problem and serving more than one device per resource block [3].

Although in many works mMIMO is classified as an orthogonal technique, allocating the signal from devices in the same resource block, possible by spatial diversity, allows us to

This work was partly supported by The National Council for Scientific and Technological Development (CNPq) of Brazil under Grants 310681/2019-7, partly by the CAPES- Brazil - Finance Code 001, and the Londrina State University - Paraná State Government (UEL).

T. A. Bruza Alves and Taufik Abrão are with the State University of Londrina (UEL), Department of Electrical Engineering, Londrina-PR, E-mails: thiagobruza@hotmail.com, taufik@uel.br

classify it as a non-orthogonal technique too [4]. There is a vast literature demonstrating the superior performance of the Spectral Efficiency of NOMA when compared to Orthogonal Multiple Access (OMA) techniques [5]. Previous aims to improve the communication system performance by combining MIMO (with a small number of antennas M) and NOMA have been discussed in [6]–[9].

Studies comparing NOMA and mMIMO in a single cell are proposed in [4], [10], [11]. The acquisition of Channel State Information (CSI) through pilot acquisition to NOMA system is proposed in [10]. In [11], the application of NOMA in the mMIMO scheme is proposed, and better results are achieved in the proposed comparative. Moreover, in [4] is analyzed the performance of NOMA and mMIMO in line of sight and non-line of sight.

The canonical mMIMO refers to the systems with BSs formed by a large number of antennas M when compared to the number of active devices, K , succinctly $M \gg K$ is considered a mMIMO setup. The typical NOMA improves the SE by superposing the signals of the selected devices to form a cluster in the power domain, multiplexing it over the same signal and served by the same beamforming. Nonetheless, the success of NOMA depends on the Successive Interference Cancellation (SIC).

Power-domain NOMA can be a candidate technology in dense networks [12]. To improve performance and minimize the impact to assume the perfect SIC [13], devices are divided into two groups. After grouping in pairs and forming a cluster, each pair forms a cluster with a high difference between channel conditions. The device with a higher channel condition can decode the signal sent to the device with the lower channel condition. The interference can thus be eliminated by SIC. The use of NOMA in BS equipped with a large number of antennas was investigated in terms of SE [4], [10] we propose in a similar configuration system increasing the loading up to 2 times the number of antennas in BS and analyze the SE, EE, and SE-EE trade-off.

The EE metric is a popular figure of merit employed to analyze the balance between power consumption and data rate. The EE is the ratio between the effectively transmitted data rate and the total power expended during the transmission process, including instantaneous and static components. With the EE metric, it is possible to evaluate the efficiency with which a system uses the limited energy resource to communicate data and optimize this ratio. Can show the tendency of energy consumption in the case of seeking justice among devices.

The Zero Forcing (ZF) is simple and popular alternative interference suppression beamforming under perfect CSI condition and achieving a satisfactory condition in real situations when imperfect CSI, in this work, we adopt perfect CSI, for

that the pilots are needed. The adoption of NOMA system with a large number of antennas requires a defined equivalent channel to be deployed for interference mitigation; and according to the NOMA principle, makes the equivalent channel matrix smaller than the original one due to the exploration of power domain in NOMA.

Various transmission topologies already deal with the EE problem in mMIMO, finding the optimal number of antennas, number of devices in a cell, and the maximal EE [2], [14]. The EE analysis in the NOMA system is carried out in [15], and its superiority is demonstrated when compared with conventional orthogonal multiple access (OMA) systems. Recent researches seek to improve the NOMA performance, e.g. in [16], the minimum pairing distance is defined and compared to the OMA, while in [17] it's presented a comparison between OMA and cell-free system equipped with mMIMO-NOMA. An EE analysis in Terahertz (THz)-NOMA-Multiple-Input Multiple-Output (MIMO) was proposed in [18]. Still, the number of active devices is much smaller than the number of antennas in the BS, and [19] is a survey about Power Domain NOMA and makes clear the vacuum of EE analysis and comparison between NOMA with many antennas and mMIMO.

Recent works propose the deployment of NOMA combined with other techniques a more effective transmission scheme; e.g., in [20] NOMA and mMIMO are jointly considered in a two-tier network for accommodating colossal traffic. Furthermore, in [21], authors apply NOMA in *Distributed Antenna Systems* (DAS), aiming to achieve better performance when compared to the conventional NOMA or DAS technique alone. While [22] shows an in-depth survey of the state-of-the-art of power-domain NOMA variants; moreover, several open issues and research challenges of NOMA-based applications are systematized. The NOMA system presents drawbacks, such as hardware (including SIC) complexity, channel feedback, receiver design, and careful power and pilot allocation strategies [12], [19], [23].

This work focus on revealing the advantages of applying the mMIMO scheme *versus* NOMA scheme with a massive number of BS antennas, and varying the loading of devices, i.e., the ratio of the number of mobile devices to the number of BS antennas, $\rho = \frac{K}{M}$, while we change the PA strategy. Besides, we adopt a realistic model for the system's power consumption as in [2] but adapted to our needs, aiming at providing a suitable analysis of the system resource allocation.

Contributions: the contributions of this work are fourfold. **a)** an extensive and comparative analysis on the spectral efficiency (SE) performance of mMIMO system against NOMA system, varying the system loading under specific (three different) power allocation methods and making use of the area under the SE ($\mathcal{S}^{\text{SYST}}$) curve of the system as an effective, useful and fair metric of performance and efficiency; **b)** we develop an energy efficiency (EE) analysis using a detailed model of energy consumption, with fixed and variable terms related to circuitry power consumption with number of antennas and devices, respectively, providing an extensive and comparative analysis on both the NOMA and mMIMO systems under realistic operation scenarios and making use of the area under the EE ($\mathcal{E}^{\text{SYST}}$) curve of system; **c)** an analysis on the SE-EE trade-off is developed considering a wide range of loading of devices, verifying the fairness between devices; **d)** finally, under mild conditions, we provide evidences for the NOMA's ability to serve a greater number of devices than mMIMO system.

The remainder of the paper is organized as follows. Section II describes the system models for NOMA and mMIMO

adopted in this work. In Section III we present the proposed EE-SE formulation for NOMA and massive MIMO systems. Numerical results are analyzed in IV. Section V concludes the paper.

Notation. In this work, boldface lower case and upper case characters denote vectors and matrices, respectively. The operator $(x)^+ = \max(0, x)$. The operators $[\cdot]^T$, $\mathbb{E}[\cdot]$ and $|\cdot|$ denote transpose, expectation and cardinality, respectively. A random vector $\mathbf{x} \sim \mathcal{CN}\{0, \mathbf{I}_m\}$ is circularly symmetric Gaussian distributed with mean 0 and covariance matrix \mathbf{I}_m . \mathbf{I}_m is $m \times m$ identity matrix.

II. SYSTEM MODELS

Let us consider a multi-user single-cell Downlink (DL) transmission operating in a Time Division Duplex (TDD) with K single-antenna active devices, communicating with one BS, which is equipped with M transmit antennas in Non-Line-Of-Sight (NLOS). The set \mathcal{K} is formed by K devices, these devices are randomly distributed in a radius disk d_{\max} , the disk area is formed by two sub-disk with the same number of devices in each sub-area; both subsets are identified as \mathcal{K}_H and \mathcal{K}_L . In the first subset, \mathcal{K}_H represents devices' indexes having the higher channel coefficient and sort in descending order, while the other subset \mathcal{K}_L are formed by the devices with lower channel coefficient and sort in ascending order; the indexes $k \in \mathcal{K}_H$ and $k \in \mathcal{K}_L$ such that:

$$\begin{aligned} \mathcal{K} &= \mathcal{K}_H \cup \mathcal{K}_L, \quad \text{where} \\ \mathcal{K}_H &= \{1, \dots, K/2\} \quad \text{and} \quad \mathcal{K}_L = \{K/2 + 1, \dots, K\}. \end{aligned} \quad (1)$$

The channel vector modeling of device k can be described liked as:

$$\mathbf{h}_k = \sqrt{\beta_k} \mathbf{h}'_k, \quad k = 1, \dots, K, \quad (2)$$

where β_k is the large-scale fading coefficient and satisfy

$$\beta_j > \beta_i, \quad \forall j \in \mathcal{K}_H, \quad \forall i \in \mathcal{K}_L. \quad (3)$$

Herein, the pathloss model in [dB] is defined as:

$$\beta_k = \beta_0 + 10 \cdot \xi \cdot \log_{10}(d_k), \quad (4)$$

where d_k is the distance of user k to BS, ξ is the pathloss coefficient, and β_0 is the attenuation at the distance of reference.

In each coherence interval, \mathbf{h}'_k in (2) for device k is an independent random small-scale fading realization from an independent Rayleigh fading distribution, $\mathbf{h}'_k \sim \mathcal{CN}(0, \mathbf{I}_M)$, $k = 1, \dots, K$. The transmitted signal $\mathbf{x}_k \in \mathbb{C}^M$ is the beamformed data symbol of device k :

$$\mathbf{x}_k = \mathbf{g}_k \sqrt{p_k} s_k, \quad (5)$$

where \mathbf{g}_k is a normalized beamforming vector, p_k normalized transmission power and $s_k \sim \mathcal{CN}(0, 1)$ is the data symbol of device k , and period T_s . The signal received at the k -th device:

$$\begin{aligned} y_k &= \sum_{k'=1}^K \mathbf{h}_k^T \mathbf{x}_{k'} + n_k, \\ &= \sqrt{\beta_k} \mathbf{h}'_k{}^T \sum_{k'=1}^K \mathbf{g}_{k'} \sqrt{p_{k'}} s_{k'} + n_k, \\ &= \sqrt{\beta_k p_k} \mathbf{h}'_k{}^T \mathbf{g}_k s_k + \sqrt{\beta_k} \mathbf{h}'_k{}^T \sum_{\substack{k' \neq k \\ k'=1}}^K \mathbf{g}_{k'} \sqrt{p_{k'}} s_{k'} + n_k, \end{aligned} \quad (6)$$

where $n_k \sim \mathcal{CN}(0, 1)$ is the additive noise. Notice that this modeling applies to both NOMA and mMIMO systems, but beamforming is selected differently, and this topic will be addressed in the next sections.

A. Prior Actions

Because the BS needs to know *a priori* crucial information related to the channel and devices distributed in the cell, including device location, rate demanded, and channel coefficient, such required *a priori* information may differ depending on the multiple access scheme considered [12].

The option for the mMIMO and NOMA systems was carried out with the guarantee that the needs of the devices would be met, and this initial step was carried out successfully. Subsection III-E briefly discusses the preliminary information required to proceed with different Power Allocation (PA) procedures in both mMIMO and NOMA systems.

B. Pilot Overhead for Channel State Information

Fig. 1 compares the pilot-data transmission structure along the one-channel coherence interval for both mMIMO and NOMA systems considered. Notice that T_s is the time required to transmit a data symbol (Data). Moreover, the channel coherence time interval T is assumed to be a multiple of the Data symbol period, $T = \nu \cdot T_s$. The power allocated to each pilot in the training step is enough. In contrast, the number of pilots, and the dedicated portion of coherence interval for data transmission are assumed to be the same in both systems.

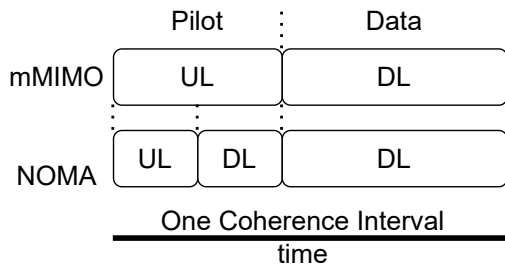


Figure 1: Coherence time interval structure: the training and data transmission structure for mMIMO and NOMA schemes under TDD NLOS setup.

Notice that in NOMA transmission, the pilot transmission step is split into two portions, half for the UL transmission pilots and receive the DL pilot confirmation; this happens because to perform SIC, the cell-center devices need to learn the effective channels that are established by the beamforming. Additionally, the beamforming vectors are based on cell-center devices, producing limited rates achieved in cell-edge devices. On the other hand, in the mMIMO scheme, a significant advantage is that there is no need for DL pilots since the effective channels created by the beamforming are highly predictable, *i.e.* nearly deterministic gain and phase due to channel hardening effect [4].

Assumption 1: In the NOMA system, the power allocated to each downlink pilot is sufficient to reach the destination device.

C. Beamforming for NOMA and mMIMO systems

At the mMIMO system, each device is served by a single beamforming vector. The ZF technique is a popular interference-suppressing beamforming scheme in the mMIMO system since it eliminates all inter-user interference using individual beamforming for each device, while the favorable propagation facilitates such interference suppressing in massive MIMO configurations. Besides, to perform ZF precoding in NOMA system, it is essential to understand the NOMA *user-pairing* concept.

User-pairing: Inherent to the NOMA system, user clustering can be performed in several ways after the *user-sorting* and the user classification in center-users and edge-users subsets. Because we know that the SE of NOMA is directly proportional to the difference between the pathloss of the users, a natural choice consists in pairing users with as higher as possible pathloss differences [6]:

$$\Delta\beta_k = \beta_k - \beta_{K+1-k}, \quad (7)$$

forming the cluster k for $k = 1, \dots, K/2$. With the pair formed, carefully beamforming vectors selection is required. Hence, in NOMA we assume that the *beamforming vector* for paired users is the same, *i.e.*, $\mathbf{g}_k = \mathbf{g}_{K+1-k}$ for all $k = 1, \dots, K/2$.

Assumption 2: In *user-pairing* procedure, we assume that the paired users are aligned with the BS so that the same beamforming can serve all paired users simultaneously. Hence, by admitting that each pair of devices is spatially aligned with the BS, and using localizing tools described, for instance, in [23], [24], one should assume further *a priori user-pairing* step in NOMA systems.

Assumption 3: In NOMA system, beamforming serves more than one aligned device simultaneously; specifically, in this paper, two aligned devices per cluster are admitted according to the *user-pairing* step, while eliminating the inter-cluster interference (favorable propagation) under adopted perfect CSI conditions.

In this work we adopt the linear ZF precoding as defined by the vector:

$$\mathbf{g}_k = \mathbf{h}'_k (\mathbf{h}'_k \mathbf{h}'_k)^{-1}, \quad (8)$$

and satisfying $\mathbf{h}'_i \mathbf{g}_k = 0, \forall i \neq k$, *i.e.*, the favorable propagation effect between users belonging to distinct clusters.

III. SE-EE IN NOMA AND mMIMO SYSTEMS

We discuss the SE and EE configurations in the NOMA and mMIMO systems. The operation of the NOMA system requires pairing devices so that the channel coefficients of the devices in the same cluster must be appropriately different, enabling power domain usage. As already mentioned, the interference cancellation process via beamforming presents problems that we will demonstrate below.

A. Data Rates in NOMA with ZF

Devices are divided into two sets like described in Eq. (1), and these groups are represented by Eq. (9) by their large-scale fading coefficient and are grouped into pairs forming a cluster as Fig. 2, the cluster k is formed by one device in cell center set \mathcal{K}_H and one device in cell edge set \mathcal{K}_L . Hence, the devices are grouped into two subsets:

$$\begin{aligned} \mathcal{K}_H &= \{\beta_1 > \beta_2 > \dots > \beta_{k/2}\}, \quad (\text{center devices set}) \\ \mathcal{K}_L &= \{\beta_K < \beta_{k-1} < \dots < \beta_{k/2+1}\}. \quad (\text{edge devices set}) \end{aligned} \quad (9)$$

The *user-pairing* adopted in Eq. (9) is the same as proposed in [6], creating the largest possible difference in channel coefficients for devices not yet paired.

Assumption 4: In this paper, we assume perfect SIC, and only one perfect SIC stage per cluster is performed, since just 2 devices per cluster are admitted.

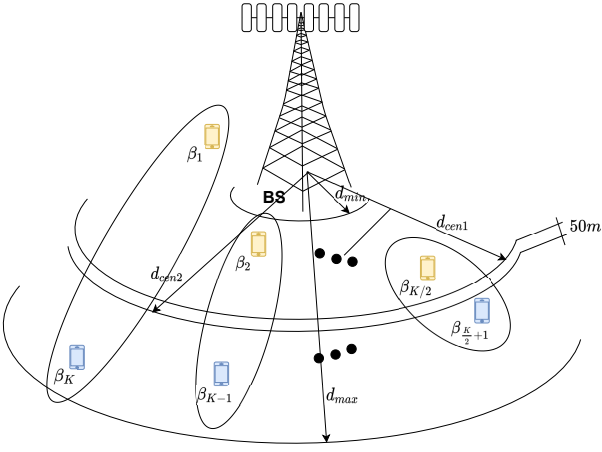


Figure 2: System Model indicating the Paring formation in NOMA system. Both mMIMO and NOMA systems deploy the same massive number of antennas at base-station, M .

The instantaneous Signal to Interference plus Noise Ratio (SINR) of devices in cluster k is defined as:

$$\text{SINR}_k = \frac{\beta_k p_k |\mathbf{h}'_k \mathbf{g}_k|^2}{\beta_k \sum_{k' \neq k}^K p_{k'} |\mathbf{h}'_k \mathbf{g}_{k'}|^2 + 1}. \quad (10)$$

In each cluster, the cell-edge devices treat the interference as noise and decode their data symbols, whereas the cell-center device can decode the data symbols of the cell-edge device and perform SIC, hence effectively removing the interference due to the cell-edge device under *Assumption 3*.

To perform SIC, the cell-center device needs to be able to decode data signal intended for the cell-edge device, *i.e.*, the ergodic SINR of the cell-edge device, SINR_{K+1-k} , at device k , defined as $\text{SINR}_{k,K+1-k}$, must be greater than or equal to the ergodic SINR of the k -th cell-center device. Hence, given the uplink (mMIMO and NOMA) and downlink (NOMA) pilot overhead and assuming perfect CSI in all receivers, and admitting *Assumption 4*, the following condition must be satisfied [4], [10]:

$$\mathbb{E}[\text{SINR}_{k,K+1-k}] \geq \mathbb{E}[\text{SINR}_k], \quad (11)$$

where

$$\text{SINR}_{k,K+1-k} = \frac{\beta_k p_{K+1-k} |\mathbf{h}'_k \mathbf{g}_k|^2}{\beta_k \sum_{k' \neq K+1-k}^K p_{k'} |\mathbf{h}'_k \mathbf{g}_{k'}|^2 + 1}. \quad (12)$$

Herein, the condition in (11) must be satisfied by selecting the transmit powers appropriately.

The achievable ergodic rate of devices in cluster k , *i.e.* device k in \mathcal{K}_H subset and device $K+1-k$ in \mathcal{K}_L subset, under Assumptions 1–4, is given by the ergodic rate contribution of user-center device:

$$R_k^{\text{NOMA}} = \tau \mathbb{E} [\log_2 (1 + \text{SINR}_k)], \quad \forall k \in \mathcal{K}_H \quad (13)$$

in [bits/s/Hz], and for the user-edge device:

$$R_{K+1-k}^{\text{NOMA}} = \tau \mathbb{E} [\log_2 (1 + \text{SINR}_{K+1-k})], \quad \forall k \in \mathcal{K}_L \quad (14)$$

where $\tau = (1 - \frac{K \cdot T_s}{T})$, is the portion of each channel coherence interval (T) that is used for data transmission.

Assuming perfect channel state information, ZF precoding for inter-clusters interference elimination, and using random

matrix theory results [25], the k -th cluster NOMA achievable rate is obtained plugging eq. (10), (13) and (14):

$$R_{\text{cl-}k}^{\text{NOMA}} = \tau \mathbb{E} [\log_2 (1 + \bar{M} \beta_k p_k)] + \tau \mathbb{E} \left[\log_2 \left(1 + \frac{\beta_{K+1-k} p_{K+1-k}}{\beta_{K+1-k} p_k + 1} \right) \right], \quad (15)$$

$\forall k \in \mathcal{K}$ and $\bar{M} = M + 1 - K/2$. Hence, the NOMA system can operate until $K < 2M - 1$. A detailed derivation of the expressions on this section can be found in [4] and [10].

B. Data Rates in mMIMO with ZF

In the mMIMO system with ZF precoding the ergodic achievable rate for device k is given by:

$$R_k^{\text{M-MIMO}} = \tau \mathbb{E} [\log_2 (1 + \text{SINR}_k)], \quad [\text{bits/s/Hz}] \quad (16)$$

where SINR_k is defined in (10). Hence, the above mMIMO achievable rate equation becomes:

$$R_k^{\text{M-MIMO}} = \tau \mathbb{E} [\log_2 (1 + (M - K) p_k \beta_k)], \quad [\text{bits/s/Hz}], \quad (17)$$

where $(M - K)$ is obtained using random matrix theory, representing the coherent array gain of the received signal [25]. Under linear precoding and combiners, the mMIMO system operates consistently when $K < M$. Finally, the *average system sum-rate* (avg-sum-rate) is defined simply by:

$$\mathcal{R}^{\text{M-MIMO}} = \sum_{k=1}^K R_k^{\text{M-MIMO}} \quad \text{and} \quad \mathcal{R}^{\text{NOMA}} = \sum_{k=1}^{\mathcal{K}_H} R_{\text{cl-}k}^{\text{NOMA}}.$$

The mMIMO system equations have been thoroughly investigated in literature and can be found in [25] and [26].

C. Energy Efficiency

EE metric is the ratio of the number of effective bits of information received over the total energy consumed by the overall system to transmit and receive/decode such information. The system data rate can determine the number of effective information bits received at the destination. Power consumption required for processing the signal at the transmitter and receiver side is often neglected; in this sense, it is calculated just as proportional to the radiated transmitted power. The growth in the number of antennas in the BS and the increased number of devices in 5G systems can lead to unattainable EE goals. In general, the average EE can be expressed as:

$$\text{EE} = \frac{\sum_{k=1}^K R_k}{P_{\text{TOT}}}, \quad [\text{bits/Joule/Hz}], \quad (18)$$

where P_{TOT} is the total power consumption across the communication system. It should consider transmission power consumption, such as RF power amplifier inefficiency, baseband signal processing, and cooling, among others. Therefore, a more realistic and detailed energy consumption model is required.

Based on [2], the adopted power consumption model in our work considers two power terms: a) fixed-term; b) terms scaled with the number of antennas M and the number of devices K . The scaled terms occur because of the transceiver chains, coding/decoding, channel estimation, and precoding. Let the computational efficiency be L operations per joule in BS. We describe it as follows:

RF Power: P_{RF} is the power consumed to transmit the signal to active devices achieved the SINR target and $0 < \varpi \leq 1$ is the efficiency of the power amplifier.

Fixed consumption: P_{FIXED} is the power consumed at the BS which is independent of the number of transmit antennas and devices in the cell, is formed of term P_0 including the power consumption of backhaul infrastructure, control signaling, baseband processor, and term P_{SYN} a single oscillator used in all BS.

$$P_{\text{FIXED}} = P_0 + P_{\text{SYN}}$$

Dependence only on K : P_K is formed by the consumption to coding and modulation of information symbols to devices, represented by P_{COD} , the consumption to BS decoded the K sequences of information symbols, defined by P_{DEC} , and the received power, represented by P_{RX} , still composes this term, multiplied by K as well. In addition, a portion of the ZF precoding cost [27] depends only on K^3 .

$$P_K = K(P_{\text{COD}} + P_{\text{DEC}} + P_{\text{RX}}) + K^3 \frac{2}{3LT}$$

Dependence only on M . The term P_M represents the transmitted power (P_{TX}), hence

$$P_M = MP_{\text{TX}}$$

Dependence on K and M : the term P_{KM} is the cost of the ZF precoding (due to LU-based matrix inversion) [27], which depends on the number of devices, the number of antennas, and the vector information symbol.

$$P_{KM} = MK \frac{3+T}{TL} + MK^2 \frac{2}{TL}$$

Adding the portions, we obtain the overall power consumption of the system:

$$P_{\text{TOT}} = \frac{P_{\text{RF}}}{\omega} + P_{\text{FIXED}} + P_K + P_M + P_{KM} \quad [\text{W}]. \quad (19)$$

D. Power Allocation Strategies

In the sequel, we present three well-known and frequently applied strategies for power allocation. Still, due to the inherent characteristics of NOMA, we propose modifications on the classical water-filling (WF) algorithm to enable application in the NOMA system. Such modifications, namely Δ -WF, ensure that none of the paired devices are dropped-out without undoing the pairing of devices. To guarantee a certain level of power disparities in each paired device, the power allocation Δ -WF procedure in the NOMA system has two steps: a) first, we allocated power for the clusters; b) we allocate power between paired devices. Thereby, we could analyze the behavior of the systems and compare their results.

Notice that both mMIMO and NOMA systems deploy the same massive number of antennas at base-station, M . Hence, due to the *channel hardening* effect [1], [25] inherent to massive MIMO configuration, the small-scale fading vanishes across the M antennas equipped with a linear ZF precoding with vector as eq. (8). Hence, one can consider just the *pathloss coefficients* β_k as the main parameter in the power allocation policies of systems based on a massive number of antennas.

1) **Equal Power Allocation (EPA):** Equal Power Allocation (EPA) power allocation is deployed as a simple, naive strategy, where all devices are served with the same power. In mMIMO, all devices are served with the same transmission power regardless of their distance from the BS. In NOMA, power allocation has two steps. In the first step, the power is allocated equally between the pairs, and then we allocate each device's

power equally. The EPA strategy applied to mMIMO can be defined by:

$$p_k = \frac{P_{\text{RF}}}{K} \quad [\text{W}], \quad \forall k \in \mathcal{K}. \quad (20)$$

In the case of EPA procedure applied to NOMA, it is composed of two steps: in the first step, power reference to each cluster can be defined simply as:

$$p_{\text{ref}}^{\text{cl}} = \frac{2 \cdot P_{\text{RF}}}{K} \quad [\text{W}], \quad \forall k \in \mathcal{K}_H. \quad (21)$$

In the second step, the power allocation among the devices in the same cluster is defined as:

$$p_k^{\text{cl-}k} = p_{K+1-k}^{\text{cl-}k} = \frac{p_{\text{ref}}^{\text{cl}}}{2}. \quad (22)$$

2) **Proportional Channel Inversion Power Allocation (PICPA):** is another power allocation technique adopted in this study. Unlike the EPA technique, which applies the same power to all devices, PICPA applies more power to devices with the worst channel conditions, favoring fairness across the devices. Such power allocation penalizes the average sum rate in favor of fairness among all users.

The Proportional to the Inverse of the Channel Power Allocation (PICPA) strategy applied to mMIMO can be defined as:

$$p_k = P_{\text{RF}} \frac{\beta_k^{-1}}{\sum_{k=1}^K \beta_k^{-1}} \quad [\text{W}], \quad \forall k \in \mathcal{K}, \quad (23)$$

while the PICPA procedure applied to NOMA follows two steps; in the first step, the power is allocated equally among the $K/2$ clusters:

$$p_{\text{ref}}^{\text{cl}} = \frac{2 \cdot P_{\text{RF}}}{K} \quad [\text{W}], \quad \forall k \in \mathcal{K}_H, \quad (24)$$

after that, the power of each device within the k -th cluster is defined by allocating more power to the device with smaller large-scale fading β_k :

$$p_k^{\text{cl-}k} = p_{\text{ref}}^{\text{cl}} \frac{\beta_{K+1-k}}{\beta_k - \beta_{K+1-k}}, \quad \text{and} \quad p_{K+1-k}^{\text{cl-}k} = p_{\text{ref}}^{\text{cl}} - p_k^{\text{cl-}k}, \quad (25)$$

where $p_k^{\text{cl-}k}$ is the power allocated to the device k in the $\text{cl-}k$ cluster, and $p_{K+1-k}^{\text{cl-}k}$ is the power allocated to the device $(K+1-k)$, also belonging to the k -th cluster.

3) **Classical Water-Filling (WF) Algorithm:** The application of the Water-Filling (WF) algorithm in mMIMO system results in an optimal (maximum) system sum-rate solution. However, some devices are dropped out of the service due to the deteriorated channel condition. The WF power allocation strategy for mMIMO is described as:

$$\mu = \frac{1}{|\mathcal{K}|} \left(P_{\text{RF}} + \sum_{k=1, k \in \mathcal{K}} \frac{1}{\beta_k} \right), \quad (26)$$

$$P_{\text{RF}} = \sum_{k=1, k \in \mathcal{K}} p_k, \quad \text{where} \quad p_k = \left(\mu - \frac{1}{\beta_k} \right)^+, \quad \forall k \in \mathcal{K}$$

$$\text{and} \quad \mathbf{p} = [p_1, p_2, \dots, p_{|\mathcal{K}|}],$$

with the operator $(z)^+ = \max(0, z)$. Notice that the constrained value for the total power available is set to P_{RF} [W]. The Algorithm 1 describes the classical WF procedure.

On the other hand, the direct application of WF algorithm in the NOMA system implies harming the pair formation, *i.e.*, devices present in the \mathcal{K}_L set are effectively dropped-out of the service, undoing the pair. We propose a modification in classical WF like the following to allow some comparison.

Algorithm 1: Classical Water Filling (WF) for mMIMO

Input: $\mathcal{K}, P_{\text{RF}}, K = |\mathcal{K}|$

- 1 $\text{NP} \neq \emptyset$;
- 2 **while** ($\text{NP} \neq \emptyset$) **do**
- 3 solve Eq. (26) $\rightarrow \mathbf{p}$;
- 4 $\text{NP} \leftarrow$ identify null positions in \mathbf{p} ;
- 5 $\mathcal{K}/\{k\}_{\text{NP}} \leftarrow$ exclude from \mathbf{p} devices labeled as NP
- 6 **end**

Output: $\mathbf{p} = [p_1, p_2, \dots, p_{|\mathcal{K}|}]$

4) Δ -WF for NOMA: The application of classical WF in NOMA in the same way as it is applied to mMIMO causes some formed pairings to be broken, since after WF algorithm application, some devices are dropped-out from the system, making the NOMA power difference (Δ) in the devices of the same cluster vanish. Hence, we suggest modifying the classical WF procedure to be applied to NOMA accordingly. The steps of the Δ -WF algorithm are described as follows.

In NOMA, the power allocation has two steps, in the first step, the allocation is between clusters. Hence, to prevent the formed pairs from being broken, we propose the application of WF based on the large-scale fading differences of the paired devices, as defined in eq. (7): $\Delta\beta_k = (\beta_k - \beta_{K+1-k})$ inside each \mathcal{K}_L and \mathcal{K}_H subsets, eq. (9). In the second step of the procedure, the power is allocated between the devices inside the group, assuming perfect successive interference cancellation (SIC); for this to be possible, the condition in Eq. (11) must be satisfied. The new water-level in the modified Δ -WF power allocation strategy for NOMA is defined by

$$\mu = \frac{2}{\mathcal{K}_H} \left(P_{\text{RF}} + \sum_{k=1, k \in \mathcal{K}_H}^{|\mathcal{K}_H|} \frac{1}{\Delta\beta_k} \right), \quad (27)$$

$$P_{\text{RF}} = \sum_{k=1, k \in \mathcal{K}_H}^{|\mathcal{K}_H|} p_{\text{cl-}k}, \quad \forall k \in \mathcal{K}_H$$

$$\text{where } p_{\text{cl-}k} = \left(\mu - \frac{1}{\Delta\beta_k} \right)^+,$$

$$\text{and } \mathbf{p}_{\text{cl-}k} = [p_1, p_2, \dots, p_{|\mathcal{K}_H|}],$$

In the second step, the power allocation to both devices in the k -th cluster is defined as:

$$p_{K+1-k}^{\text{cl-}k} = p_k^{\text{cl-}k} = \frac{p_{\text{cl-}k}}{2} \quad (28)$$

Algorithm 2 summarize the proposed Δ -WF power allocation procedure, aiming to improve the SE of NOMA systems.

Algorithm 2: Δ -WF (modified) for NOMA systems

Input: $\mathcal{K}_H, \mathcal{K}_L, P_{\text{RF}}$

- 1 $\text{NP} \neq \emptyset$;
- 2 **while** ($\text{NP} \neq \emptyset$) **do**
- 3 solve Eq. (27) $\rightarrow \mathbf{p}_{\text{cl-}k}$;
- 4 $\text{NP} \leftarrow$ identify null position in $\mathbf{p}_{\text{cl-}k}$;
- 5 $\mathcal{K}_H/\{k\}_{\text{NP}} \leftarrow$ exclude from $\mathbf{p}_{\text{cl-}k}$ devices labeled as NP
- 6 **end**

Output: $\mathbf{p}_{\text{cl-}k} = [p_1, p_2, \dots, p_{|\mathcal{K}_H|}]$

Complexity analysis: In a comparative analysis of complexity, the Δ -WF algorithm for power allocation in NOMA system (Algorithm 2) performs two simple additional operations compared to the classical WF procedure (Algorithm 1): a) in eq.

(27) the subtraction in $(\beta_k - \beta_{K+1-k})$; and b) the division by two in (28). Besides, NOMA vs. mMIMO systems require different *a priori* information to proceed accordingly with the PA procedure.

E. Prior Information for Power Allocation Step

For implementing the PA policies, prior information is required at the BS, as defined in Table I. Some of this necessary information can be obtained through the dedicated *pilot* transmission step, at the cost of some overhead, as described in Section II-B. Moreover, a preliminary step is known, in which the *spatial localization* and *path loss* estimation of all devices must be realized. With such *a priori* information availability, the *user-sorting* and *user-pairing* steps can be performed.

Table I: Prior information required to PA procedure

PA		β_k	h_k^l	K	\mathcal{K}_H	\mathcal{K}_L	p_k , eq.
EPA	mMIMO	—	—	▲*	—	—	(20)
	NOMA	—	—	▲	—	—	(21), (22)
PICPA	mMIMO	▲*	—	—	▲*	▲*	(23)
	NOMA	▲	—	—	▲*	▲	(24), (25)
WF	mMIMO	▲*	—	—	▲*	▲*	(26), Alg. 1
Δ -WF	NOMA	▲	—	—	▲*	▲	(27, 28), Alg. 2

▲ information needed a prior

* obtained via Pilot Overhead

— Information not needed

IV. NUMERICAL RESULTS

The numerical evaluations for the proposed analyses of NOMA and mMIMO systems are presented in this section. The simulation system and channel parameter values deployed along this section are depicted in Table II. The BS is located at the center of cell and equipped with massive M BS transmit antennas in typical non-line-of-sight (NLOS) channel propagation scenario. At the same time, the devices are randomly distributed in the cell area and split into two subsets, \mathcal{K}_L and \mathcal{K}_H , as illustrated in Fig. 2. In all simulations, we consider a block fading model where the time-frequency resources are divided into coherence time intervals (T), in which the channels remain constant and frequency flat, and it is measured in multiple of symbol transmit period (T_s). The system and channel scenarios have been simulated using Matlab 2019 software running under one Intel HD Graphics 6000 GPU, Intel(R) Dual-Core(TM) I5 CPU @ 1.6 GHz, and 8 GB RAM.

Table II: Simulation Parameters

Parameter	Value
BS antennas	$M = 64, 128$ and 256
Max. # Devices in the cell	$K = \zeta \cdot M$ (NOMA) $K = M$ (mMIMO)
Cell loading	$\rho = K/M$
Total RF power available	$P_{\text{RF}} = 1\text{W}$
Pairs NOMA / Clusters	$N = K/\zeta = K/2$
NOMA devices per cluster	$\zeta = 2$
# antennas per device	1
Cell edge length	$d_{\text{max}} = 350$ m
Strong device position	$[d_{\text{min}}; d_1] \in [50; 100]$ m
Weak device position	$[d_2; d_{\text{max}}] \in [150; 350]$ m
Array gain MIMO device	$M - K$
Array gain NOMA k_H	$M + 1 - K/2$
Data symbol period	T_s
Coherence time interval	$T = 512 \cdot T_s, \quad \iota = 512$
Channel	
Pathloss exponent	$\xi = 3.78$
Attenuation at a d_0 reference	$\beta_0 = 130$ [dB]
# Monte-Carlo realizations	1000

A. Spectral Efficiency Comparison

The mMIMO and NOMA SE performance analysis is carried out in this subsection, by increasing the number of devices two by two until the loading limit $\rho = 2$. The results consider $M = 64, 128$ and 256 BS antennas. In Fig. 3. (a) the results of SE are achieved when the RF power available is allocated following the EPA strategy, where each device receives the same PA values. The mMIMO system overcame NOMA in all situations when the loading $\rho < 0.6$. However, the NOMA system achieves a higher SE than the mMIMO for each M scenario when the loading of devices increases, $\rho > 0.6$. The maximum avg-SE is 373 [bits/s/Hz], being attained with ZF-NOMA $M = 256$ antennas and $\rho \approx 0.76$. Besides, one can infer that the mMIMO does not work with a loading higher than 1, due to the array gain reaching 0 at full loading of devices, while NOMA works suitably until the loading attains $M \cdot \zeta$, where ζ is number of devices per cluster.

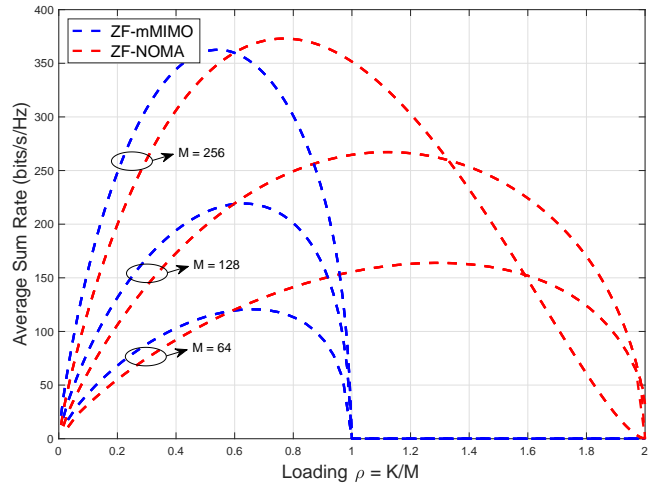
Fig. 3.(b) depicts the results of SE achieved in the mMIMO and NOMA systems when the PICPA method is applied to allocate the available RF power per device along the BS antennas. The maximum avg-SE in mMIMO system overcomes the NOMA counterpart until the loading ρ exceeds ≈ 0.62 for the three BS antenna configurations, $M = 64, 128$, and 256 . This PA technique provides more power to devices with the worst channel condition, making the SE result reach maximum values below the EPA.

Fig. 3.(c) depicts the conventional WF algorithm applied to mMIMO. Under such a power allocation approach, we highlight that forming pairs is unfeasible in the NOMA system. Indeed, the WF algorithm can maximize the system SE since it allocates more power to devices with better channel conditions. In contrast, devices under bad channel conditions (below the water level) are dropped out of the service.

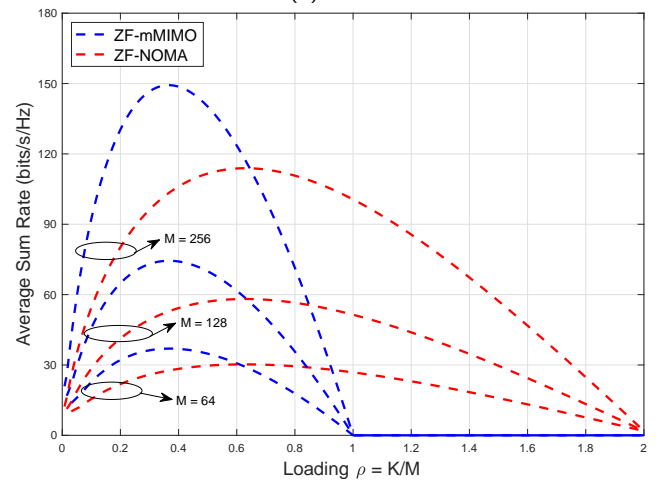
The classical WF algorithm has been adapted to the NOMA system dropped-out always a pair of devices. Such adaptation reveals substantial improvements of avg-sum-rate when M is low compared to classical WF PA in mMIMO. The Δ -WF power allocation procedure preserves the pairs clustering formation in the NOMA system, allocating more power to the cluster with a higher difference between coefficients of large-scale fading. Fig. 3.(c) shows that the maximum avg-SE ≈ 361 [bits/s/Hz], which is achieved under $\rho = 1$ ($K \approx 256$ devices) when the modified WF is deployed in NOMA system. Moreover, when the number of BS antennas is lower ($M = 64$ or 128), the NOMA achieved a peak higher than mMIMO, e.g., for $M = 64$ antennas, the peak of SE mMIMO occurs at loading $\rho \approx 0.7$, while the NOMA SE peaks at $\rho \approx 1.2$. However, as the number of BS antennas grows, the NOMA SE advantage decreases.

Number of active devices after PA procedure. Fig. 4 shows the number of actives device after applying PA methods: in the EPA and PICPA algorithms, all devices remain activated. However, in classical WF mMIMO system when the number of device increases beyond $\rho \approx 0.25$, half of the devices are dropped-out; while in Δ -WF NOMA PA, the percentage of active devices is always higher, e.g. higher than 70% for $\rho \approx 1.1$ and $M = 256$ antennas, the worst case.

Fig. 5 summarizes avg-sum-rate surfaces in terms of SE $\times \rho \times M$ results achieved by NOMA with EPA, mMIMO with WF, and NOMA with modified Δ -WF. In the initial loading part, $\rho < 0.65$, the classical WF PA in ZF-mMIMO achieves better results until the loading (pink surface). When the number of antennas is low as $M = 64$ and ρ is in between 0.7 and 1.8, the EPA PA applied to NOMA (green



(a) EPA



(b) PICPA

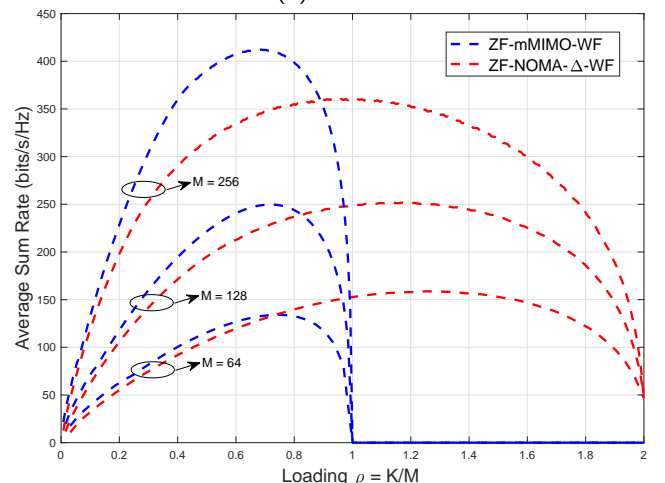
(c) Classical WF in ZF-mMIMO and Δ -WF in ZF-NOMA

Figure 3: The average sum-rate with the loading of devices $0 < \rho < 2$, considering four power allocation methods: EPA, PICPA, WF, and Δ -WF. The average is obtained over 1000 random devices locations.

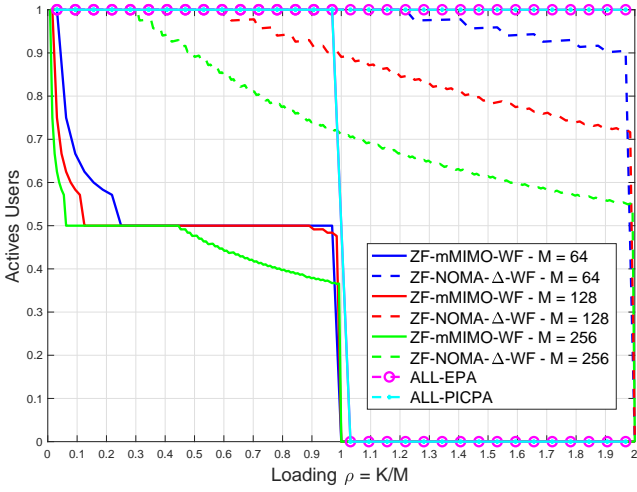


Figure 4: The average of active devices after PA procedure versus loading of devices in the range $0 < \rho \leq 2$. The average is obtained over 1000 random devices locations.

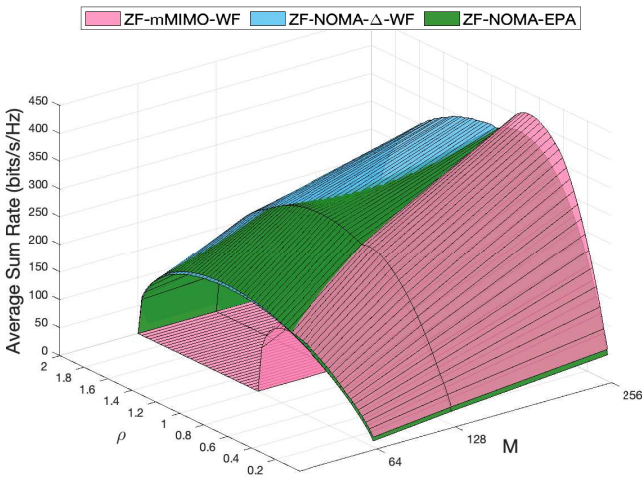


Figure 5: Average sum rate with loading ρ and M .

surface) achieved superior results. Moreover, when $M = 128$ and $0.8 < \rho < 1.6$, the ZF-NOMA-EPA achieve superior results (green surface). For a higher number of antennas in BS, *i.e.*, $M = 256$ only in a short loading of devices range, $0.86 < \rho < 0.97$, the ZF-NOMA-EPA achieves superior SE results. Finally, when $\rho > 0.97$, the modified Δ -WF achieves competitive results (blue surface).

B. Jain's Fairness Index

Another critical analysis developed was to analyze the fairness between the devices, *i.e.*, to know the difference in the transmission rate achieved by active devices in the cell. For this measure, we use the Jain's Fairness index like described in [28] and can be defined as:

$$\mathcal{F}_M^{\text{SYST}} = \frac{\left(\sum_{k=1}^M R_k\right)^2}{M \sum_{k=1}^M R_k^2}. \quad (29)$$

The Fig. 6. depicts the fairness curves attainable by NOMA and mMIMO systems with EPA, PICPA, WF, and Δ -WF PA procedures when the loading of devices grows until $\rho = 2$. Fig. 6.(a) shows the Jain's Fairness Index when EPA policy is used, the mMIMO system performs better \mathcal{F} results than NOMA for $\rho < 1$, on the other hand, NOMA can attain $\mathcal{F}_M^{\text{NOMA}} \approx 0.5$ in almost every loading of devices, independent of M .

Fig. 6.(b) reveals the Jain's Fairness Index when the PICPA method is applied, despite the SE result being lower in this PA method, the mMIMO obtains the best fairness result, keeping the $\mathcal{F}_M^{\text{mMIMO}}$ consistently above 0.85, still the NOMA under 0.5.

The Jain's Fairness Index when WF and δ -WF are depicted in Fig.6(c), It is intrinsic to these algorithms to allocate more power to devices with better channel conditions, which causes fairness between devices to be impaired. In this method, it is possible to observe a significant influence of the number of antennas M in the BS and the fairness result.

C. Energy Efficiency Comparison

Energy efficiency (EE) is another important figure of merit used to compare systems' performance. In this section, a power consumption model based on fixed circuitry power part and that one varying according to the number of antennas M and the number of devices K has been adopted, following eq. (19).

Table III [2] presents the adopted parameter values for the EE analysis and comparison discussed in this subsection. Fig. 7 depicts the performance of EE with EPA, PICPA, WF, and Δ -WF PA procedures, considering the exact three quantities of antennas. Fig. 7.(a) shows the EE performance with EPA. In this method, all devices receive the same power. The avg-EE mMIMO overcomes the NOMA around 13% to 20%. It was possible to observe that adding antennas in the BS increases the power consumption, harming the EE result. Again, under loading of devices $0.6 < \rho \leq 2.0$, the NOMA overcomes the mMIMO system.

Table III: Adopted Parameters values for EE analysis [2]

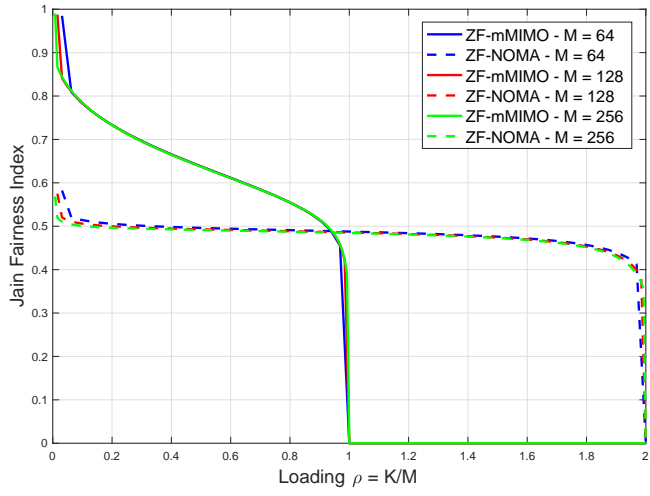
Parameter	Value
Backhaul Infrastructure	$P_0 = 2 \text{ W}$
Single oscillator	$P_{syn} = 2 \text{ W}$
Coding and modulation	$P_{COD} = 4 \text{ W per device}$
Decoding and demodulation	$P_{DEC} = 0.5 \text{ W per device}$
Receive power	$P_{RX} = 0.3 \text{ W per device}$
Transmitted power	$P_{TX} = 1 \text{ W per antenna}$
Efficiency of Power Amplifier	$\varpi = 0.3$
Operations/Joule	$L = 10^9 \text{ oper. per joule}$

Fig. 7.(b) reveals the EE performance with PICPA. In this method, more power is allocated to devices with poor channel coefficients, resulting in reduced poor EE performance for both NOMA and M-MIMO systems, attaining a maximum of 0.25 and 0.16 [bits/W] for mMIMO and NOMA, respectively. The maximum EE attained by mMIMO is generally around 50% higher than NOMA. However, for loading of devices $\rho \geq 0.65$, NOMA overcomes mMIMO EE performance.

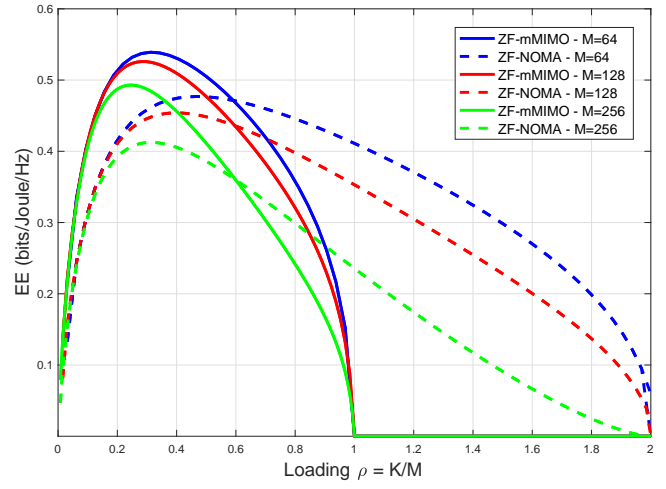
Fig. 7.(c) depicts the EE performance in the mMIMO with classical WF and in the NOMA with Δ -WF algorithm. It is possible to confirm the superiority of energy efficiency of mMIMO within the range where it operates consistently, *i.e.*, $0 < \rho < 1$. Notice that the maximum EE achieved by mMIMO is about 70 % higher than NOMA for different BS antennas. Finally, NOMA becomes more energy efficient than mMIMO only when the loading of devices is high, $\rho > 0.95$.

In all analyzed system scenarios, the mMIMO equipped with classical WF PA procedure achieves higher maximum EE. The mMIMO attains better EE results than NOMA for $\rho < 1$. On the other hand, NOMA can serve a more significant number of devices (twice) than mMIMO.

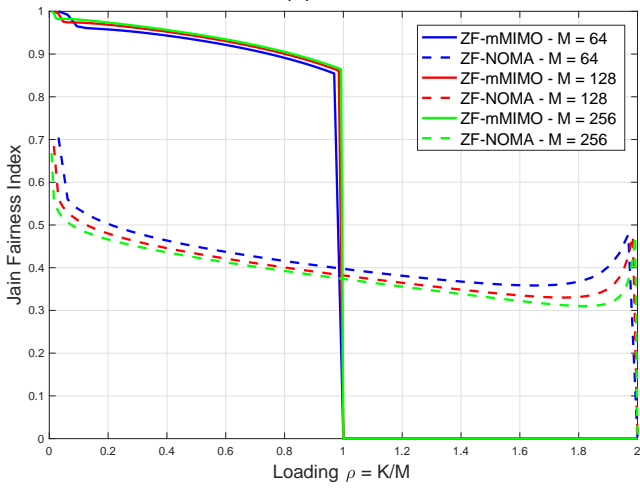
Fig. 8 summarizes the best EE results in a surface plotting for the mMIMO with WF overcoming NOMA across the entire



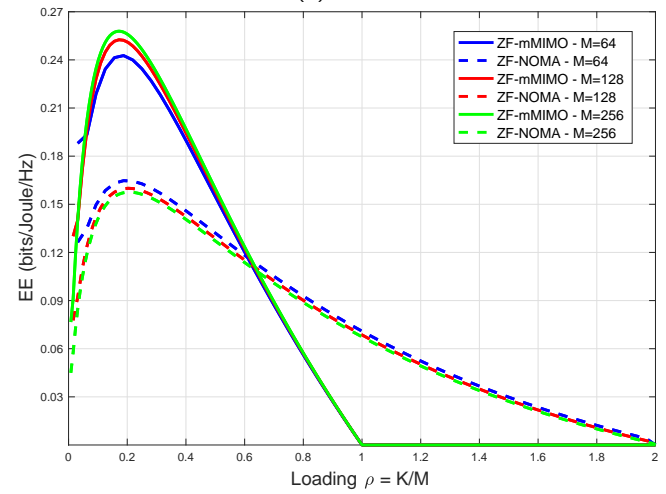
(a) EPA



(a) EPA



(b) PICPA



(b) PICPA

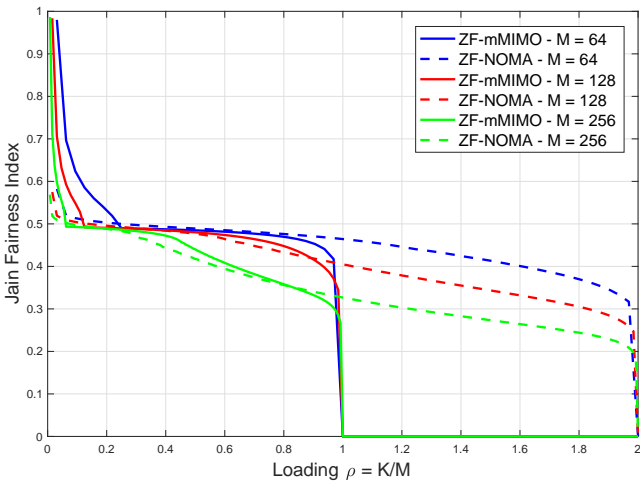
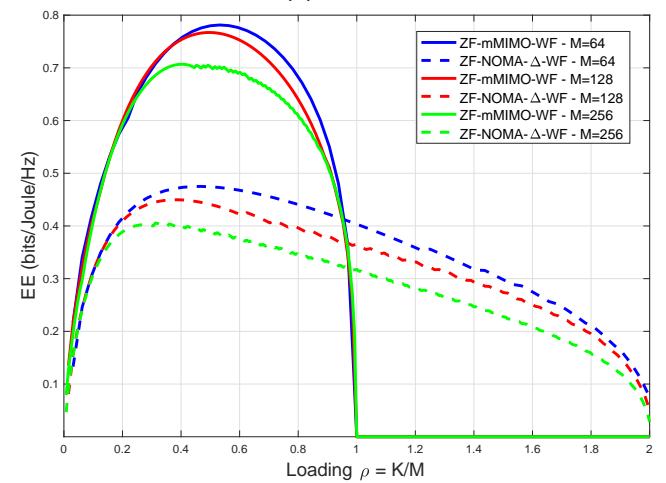
(c) WF and Δ -WF(c) WF and Δ -WF

Figure 6: The fairness of NOMA and mMIMO system under three power allocation procedures: (a) EPA; (b) PICPA; (c) WF and Δ -WF. The average is obtained over 1000 random device locations.

Figure 7: EE for NOMA vs. mMIMO under three power allocation procedures: (a) EPA; (b) PICPA; (c) WF and Δ -WF. Average EE obtained over 1000 random devices locations.

loading range where it operates consistently. For device loading $\rho > 1$, the NOMA operates under lower EE until the loading $\rho = 2$. Moreover, considering the smallest number of antennas in the BS, the NOMA with EPA overcame the NOMA with modified Δ -WF; despite that, as the number of antennas in the BS increases, the NOMA with Δ -WF achieves marginal superior EE results.

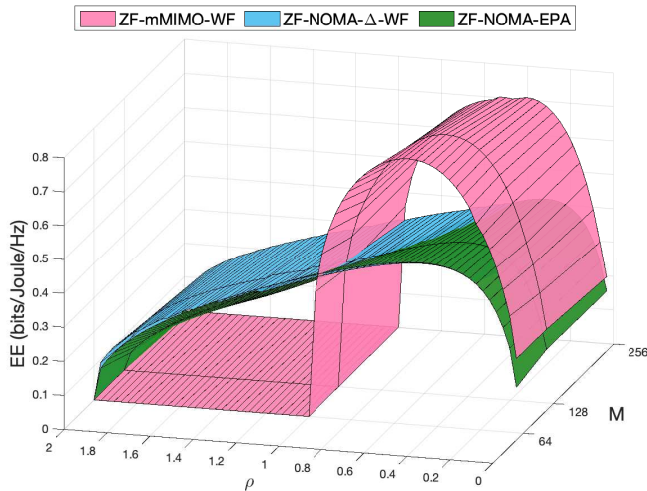


Figure 8: EE with loading ρ and M .

D. Area Under Curves SE and EE

For a fair comparison, one can consider a wide range of average SE and EE along the loading of devices, and normalized per antenna, which can be attainable by NOMA and mMIMO systems. Hence, let us consider the corresponding areas under the SE and EE curves in Fig. 3 and Fig. 7, such that:

$$\mathcal{S}_M^{\text{SYST}} = \frac{1}{M} \cdot \int_0^{\rho=2} \overline{\text{SE}}(\rho) d\rho \quad \left[\frac{\text{bits/antenna}}{\text{s} \cdot \text{Hz}} \right]$$

and

$$\mathcal{E}_M^{\text{SYST}} = \frac{1}{M} \cdot \int_0^{\rho=2} \overline{\text{EE}}(\rho) d\rho \quad \left[\frac{\text{bits/antenna}}{\text{Joule} \cdot \text{Hz}} \right],$$

respectively, where $\overline{\text{SE}}(\rho)$ is the average overall system sum-rate, and $\overline{\text{EE}}(\rho)$ is the average overall system energy efficiency achieved under specific loading of devices ρ . Hence, comparing the values of corresponding areas under the SE and EE curves of Fig. 3 and Fig. 7, we obtained Fig. 9.

From the SE perspective, and considering EPA policy, the higher area-under-SE-curve ratio gain is achieved when the number of BS antennas is $M = 64$:

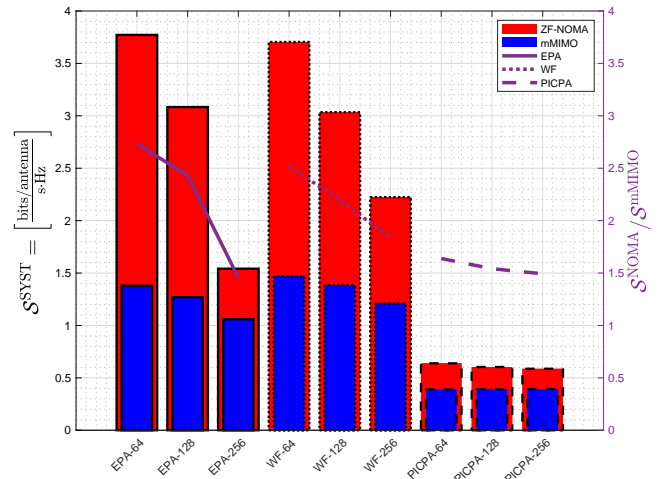
$$\mathcal{S}_{M=64}^{\text{NOMA}} \approx 2.7 \cdot \mathcal{S}_{M=64}^{\text{mMIMO}}.$$

Notice that when the number of antennas M grows, the ratio above decreases. In the same way, considering WF policy, the gain trend remains. In contrast, considering the PICPA policy, the ratio practically remains the same.

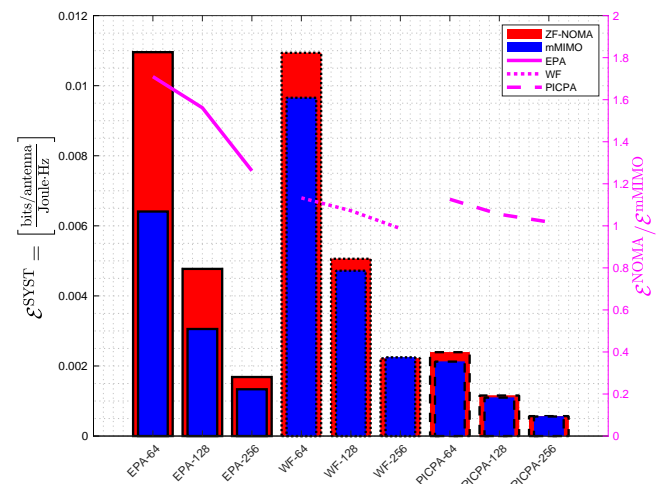
Furthermore, considering now the EE perspective, under EPA policy, the higher ratio is achieved when the BS is equipped with $M = 256$ antennas:

$$\mathcal{E}_{M=256}^{\text{NOMA}} \approx 1.8 \cdot \mathcal{E}_{M=256}^{\text{mMIMO}}.$$

As one can conclude, in almost all scenarios, NOMA is more spectrally and energetically efficient than mMIMO over an extensive range of loading of devices $0 < \rho \leq 2$, roughly, in average, 80% in terms of energy efficiency, and 170% more efficient in terms of spectral efficiency.



(a) \mathcal{S} - Bar chart of Area Under SE curves.



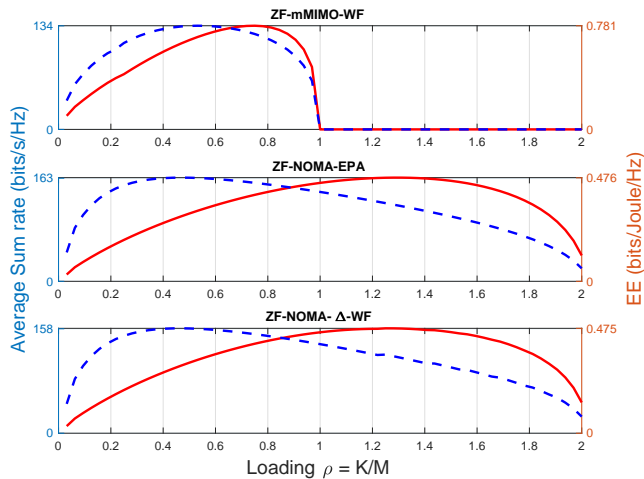
(b) \mathcal{E} - Bar chart of Area Under EE curves.

Figure 9: The Area Under curve of NOMA and mMIMO system under three power allocation procedures: (a) SE curves; (b) EE curves. The average is obtained over 1000 random devices locations.

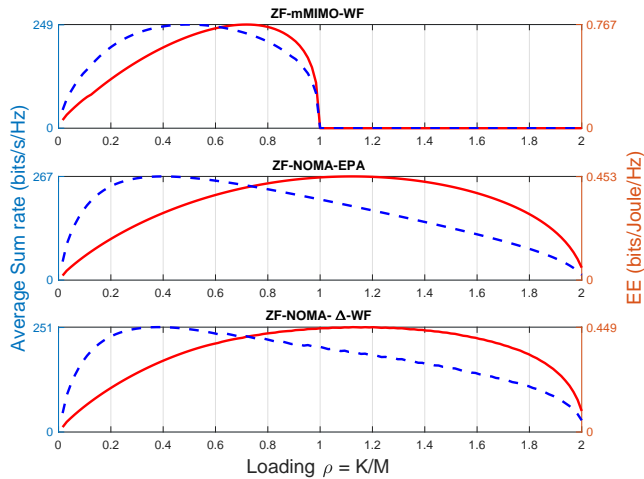
E. Resource Efficiency (SE-EE Trade-off)

The NOMA and mMIMO are analyzed in terms of SE and EE trade-off, namely *resource efficiency* (RE), considering loading of devices increasing up to 2. From Fig. 10, one can find graphically the best loading of devices range that maximizes the SE-EE trade-off for each BS antenna configuration M . The left y-axis depicts avg-SE, and the right y-axis shows the avg-EE. Table IV summarizes the optimal loading of devices that maximizes the SE-EE trade-off and shows the percentage of active users after Power Allocations and Jain's Fairness Index. Fig. 10.(a) reveals the results when $M = 64$, NOMA with EPA achieved SE-EE trade-off with the highest loading of devices and the highest SE in trade-off; on the other hand, mMIMO with classical WF achieved the highest SE-EE trade-off; however, the percentage of actives devices is around 0.5. Fig. 10.(b) depicts results when $M = 128$, NOMA with EPA achieved SE-EE trade-off with the highest loading of devices, in contrast, mMIMO with classical WF with lower loading of devices achieved higher values of SE and EE in trade-off with half of the active devices. Fig 10.(c) showed the results when $M=256$, NOMA with Δ -WF achieved SE-EE trade-off with the highest loading of devices, and one more time mMIMO with WF achieved higher SE-EE trade-off with 47% of active devices. It is possible to demonstrate that the

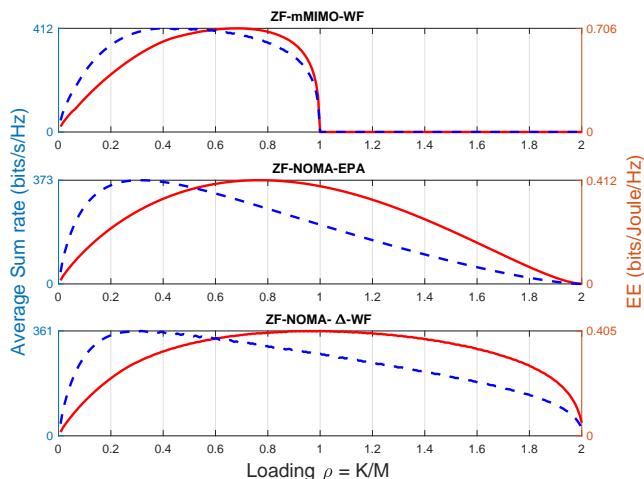
increase of antennas in the BS improves the SE result, on the other hand, it worsens the EE result.



(a) $M = 64$ BS antennas



(b) $M = 128$ BS antennas



(c) $M = 256$ BS antennas

Figure 10: SE-EE trade-off points when $M = 64, 128$ and 256 .

V. CONCLUSION AND FUTURE WORKS

This work proposes a comparative SE and EE analysis in DL single-cell between mMIMO and NOMA with BS equipped with three antenna configurations. Under the SE perspective, mMIMO with the classical WF algorithm achieved better low- and medium-loading results. On the other hand, when the

Table IV: SE-EE Trade-off

$M = 64$					
	ρ	SE	EE	Actives Users	\mathcal{F}
mMIMO-WF	0.652	131.15	0.762	.50	.485
NOMA-EPA	0.875	147.45	0.428	1.0	.485
NOMA- Δ -WF	0.844	143.48	0.441	1.0	.475
$M = 128$					
	ρ	SE	EE	Actives Users	\mathcal{F}
mMIMO-WF	0.625	243.21	0.745	.50	.475
NOMA-EPA	0.734	241.54	0.411	1.0	.49
NOMA- Δ -WF	0.703	226.32	0.405	.98	.45
$M = 256$					
	ρ	SE	EE	Actives Users	\mathcal{F}
mMIMO-WF	0.578	404.84	0.691	.47	.43
NOMA-EPA	0.523	344.70	0.380	1.0	.495
NOMA- Δ -WF	0.594	333.31	0.375	.85	.398

system loading is higher as $\rho > 0.6$ the NOMA achieves better results in the range $0.6 < \rho \leq 2$.

The analyzed PA methods applied to the NOMA system, (EPA, PICPA, and Δ -WF) result in different SE performance. Indeed, when the channel hardening condition is fully attained, and the amount of BS antennas increases ($M = 128$ and 256), the best SE results are attained with the proposed Δ -WF algorithm, but, as expected, the fairness index is harmed.

Under the EE perspective, the mMIMO achieved better results when employing the three EPA, PICPA, and WF PA methods under $K < M$. However, the NOMA can operate under higher system loading, *i.e.*, $K < 2M - 1$.

In terms of area-under-SE-curve and EE-curve metrics, \mathcal{S} and \mathcal{E} , respectively, the NOMA system attained better results, due to its ability to serve a larger number of users than mMIMO. Such numerical results confirm NOMA's ability to operate with high loading of devices. On the other hand, achieving high fairness with NOMA is impossible.

From the perspective of SE-EE trade-off, mMIMO achieved the best results, because of the superiority in EE; always achieved in loading of devices $\rho = 0.6$ in all M setups.

NOMA systems present exciting features and have been intensively investigated as a promising technique in devising future wireless generations. As future works, hybrid NOMA systems and alternative techniques such as *rate-splitting multiple access* (RSMA) can improve the overall EE of massive MIMO systems.

ACKNOWLEDGEMENT

This work was partly supported by The National Council for Scientific and Technological Development (CNPq) of Brazil under Grants 310681/2019-7, partly by the CAPES- Brazil - Finance Code 001, and the Londrina State University - Paraná State Government (UEL).

REFERENCES

- [1] E. G. Larsson, O. Edfors, F. Tufvesson, and T. L. Marzetta, "Massive MIMO for next generation wireless systems," *IEEE Communications Magazine*, vol. 52, no. 2, pp. 186–195, 2014.
- [2] E. Bjornson, L. Sanguinetti, J. Hoydis, and M. Debbah, "Designing multi-user MIMO for energy efficiency: When is massive MIMO the answer?," *2014 IEEE Wireless Communications and Networking Conference (WCNC)*, pp. 242–247, apr 2014.
- [3] Z. Ding and H. V. Poor, "Design of Massive-MIMO-NOMA with Limited Feedback," *IEEE Signal Processing Letters*, vol. 23, pp. 629–633, may 2016.
- [4] K. Senel, H. V. Cheng, E. Bjornson, and E. G. Larsson, "What Role Can NOMA Play in Massive MIMO?," *IEEE Journal on Selected Topics in Signal Processing*, vol. 4553, no. c, pp. 1–16, 2019.
- [5] A. Anwar, B.-C. Seet, M. A. Hasan, and X. J. Li, "A Survey on Application of Non-Orthogonal Multiple Access to Different Wireless Networks," *Electronics*, vol. 8, p. 1355, nov 2019.

- [6] M. S. Ali, E. Hossain, and D. I. Kim, "Non-Orthogonal Multiple Access (NOMA) for Downlink Multiuser MIMO Systems: User Clustering, Beamforming, and Power Allocation," *IEEE Access*, vol. 5, pp. 565–577, 2017.
- [7] M. Zeng, A. Yadav, O. A. Dobre, G. I. Tsiropoulos, and H. V. Poor, "Capacity Comparison Between MIMO-NOMA and MIMO-OMA With Multiple Users in a Cluster," *IEEE Journal on Selected Areas in Communications*, vol. 35, pp. 2413–2424, oct 2017.
- [8] S. M. R. Islam, M. Zeng, O. A. Dobre, and K.-S. Kwak, "Resource Allocation for Downlink NOMA Systems: Key Techniques and Open Issues," *IEEE Wireless Communications*, vol. 25, pp. 40–47, apr 2018.
- [9] X. Chen, F.-K. Gong, G. Li, H. Zhang, and P. Song, "User Pairing and Pair Scheduling in Massive MIMO-NOMA Systems," *IEEE Communications Letters*, vol. 22, pp. 788–791, apr 2018.
- [10] H. V. Cheng, E. Bjornson, and E. G. Larsson, "Performance Analysis of NOMA in Training-Based Multiuser MIMO Systems," *IEEE Transactions on Wireless Communications*, vol. 17, pp. 372–385, jan 2018.
- [11] L. Dai, B. Wang, M. Peng, and S. Chen, "Hybrid Precoding-Based Millimeter-Wave Massive MIMO-NOMA With Simultaneous Wireless Information and Power Transfer," *IEEE Journal on Selected Areas in Communications*, vol. 37, pp. 131–141, jan 2019.
- [12] B. Makki, K. Chitti, A. Behravan, and M.-S. Alouini, "A Survey of NOMA: Current Status and Open Research Challenges," *IEEE Open Journal of the Communications Society*, vol. 1, no. December 2019, pp. 179–189, 2020.
- [13] M. R. Usman, A. Khan, M. A. Usman, Y. S. Jang, and S. Y. Shin, "On the performance of perfect and imperfect SIC in downlink non orthogonal multiple access (NOMA)," *2016 International Conference on Smart Green Technology in Electrical and Information Systems (ICSGTEIS)*, pp. 102–106, oct 2016.
- [14] E. Bjornson and E. G. Larsson, "How Energy-Efficient Can a Wireless Communication System Become?," *Conference Record - Asilomar Conference on Signals, Systems and Computers*, vol. 2018-October, pp. 1252–1256, 2019.
- [15] Y. Zhang, H. M. Wang, T. X. Zheng, and Q. Yang, "Energy-Efficient Transmission Design in Non-orthogonal Multiple Access," *IEEE Transactions on Vehicular Technology*, vol. 66, no. 3, pp. 2852–2857, 2017.
- [16] S. Mounchili and S. Hamouda, "Pairing Distance Resolution and Power Control for Massive Connectivity Improvement in NOMA Systems," *IEEE Transactions on Vehicular Technology*, vol. 69, no. 4, pp. 4093–4103, 2020.
- [17] F. Rezaei, C. Tellambura, A. Tadaion, and A. R. Heidarpour, "Rate analysis of cell-free massive MIMO-NOMA with three linear precoders," *IEEE Transactions on Communications*, vol. 68, no. 6, pp. 3480–3494, 2020.
- [18] H. Zhang, H. Zhang, W. Liu, K. Long, J. Dong, and V. C. Leung, "Energy Efficient User Clustering, Hybrid Precoding and Power Optimization in Terahertz MIMO-NOMA Systems," *arXiv*, vol. 38, no. 9, pp. 2074–2085, 2020.
- [19] O. Maraqa, A. S. Rajasekaran, S. Al-Ahmadi, H. Yanikomeroglu, and S. M. Sait, "A Survey of Rate-Optimal Power Domain NOMA with Enabling Technologies of Future Wireless Networks," *IEEE Communications Surveys and Tutorials*, vol. 22, no. 4, pp. 2192–2235, 2020.
- [20] S. Rajoria, A. Trivedi, and W. W. Godfrey, "Sum-rate optimization for NOMA based two-tier hetnets with massive MIMO enabled wireless backhauling," *AEU - International Journal of Electronics and Communications*, vol. 132, no. October 2020, p. 153626, 2021.
- [21] D. Kim and M. Choi, "Non-Orthogonal Multiple Access in Distributed Antenna Systems for Max-Min Fairness and Max-Sum-Rate," *IEEE Access*, vol. 9, pp. 69467–69480, 2021.
- [22] I. Budhiraja, N. Kumar, S. Tyagi, S. Tanwar, Z. Han, D. Y. Suh, and M. J. Piran, *A Systematic Review on NOMA Variants for 5G and Beyond*, vol. 9. IEEE, 2021.
- [23] F. Zafari, A. Gkelias, and K. K. Leung, "A Survey of Indoor Localization Systems and Technologies," *IEEE Communications Surveys and Tutorials*, vol. 21, no. 3, pp. 2568–2599, 2019.
- [24] E. M. Mohamed, "Joint users selection and beamforming in downlink millimetre-wave NOMA based on users positioning," *IET Communications*, vol. 14, no. 8, pp. 1234–1240, 2020.
- [25] T. L. Marzetta, E. G. Larsson, H. Yang, and H. Q. Ngo, *Fundamentals of Massive MIMO*. Cambridge University Press, 2016.
- [26] H. Yang and T. L. Marzetta, "Performance of conjugate and zero-forcing beamforming in large-scale antenna systems," *IEEE Journal on Selected Areas in Communications*, vol. 31, no. 2, pp. 172–179, 2013.
- [27] S. Boyd and L. Vandenberghe, "Numerical linear algebra background," *[On Line]* - Available: <https://web.stanford.edu/class/ee364a/lectures/num-lin-alg.pdf>.
- [28] J. L. Jacob and T. Abrão, "Nonorthogonal multiple access systems optimization to ensure maximum fairness to users," *Transactions on*